Single 3D laser projector with speckle suppression

Lei Dong (董 磊), Anting Wang (王安廷)*, Fugui Yang (杨福桂), Shulu Wang (王书路), Lixin Xu (许立新), Chun Gu (顾 春), and Hai Ming (明 海)

Department of Optics and Optical Engineering, Anhui Key Laboratory of Optoelectronic Science and Technology, University of Science and Technology of China, Hefei 230026, China

**Corresponding author: atwang@ustc.edu.cn*

Received July 2, 2013; accepted August 20, 2013; posted online August 25, 2013

In this letter, a new single three-dimensional (3D) laser projector is proposed. As liquid crystal (LC) can produce two image patterns with orthogonal polarization states at 120 Hz, only one projector is required in this approach for reconstruction of a 3D object. The light source is made up of RGB (red, green, and blue) lasers because laser has lots of advantages such as longer life, higher brightness, and larger color gamut. A novel diffusive media with good polarization-maintaining quality is used as rear projection screen for its high transmission efficiency (∼90%) and low reflection efficiency. When laser incidents into the diffusive media, which contains lots of spherical particles with sizes between 2 and 15 μm, laser is scattered randomly and the laser speckle is reduced. A spatial phase mask is also inserted into the optical path to reduce speckle. With these techniques, the speckle contrast is reduced to 0.1 and the quality of image patterns has been greatly improved.

OCIS codes: 110.0110, 140.0140, 230.0230, 290.0290, 330.0330.
doi: 10.3788/COL201311.S21102.

Nowadays, three-dimensional (3D) display technology has been used widely in aerospace, military, medical, design, and entertainment due to its possibility of providing comprehensive information of object in the 3D sense of depth[1,2]. Most of the 3D display products based on binocular disparity in the market are polarization-based style and shutter-based style. In cinemas, polarization-based style 3D display equipment with two projectors are used very popularly but there are many disadvantages. For example, two projectors are expensive, it's very cockamamie to synchronize the two electrical signals and overlap the two optical paths, and the silver screen with good polarization-maintaining quality is very expensive. So it's not appropriate for home use. To meet this challenge, shutter glasses have been used to replace polarization glasses. With a receptor in the glasses, the liquid crystal (LC) shutter glasses can alternately accept the corresponding images in different eyes. But there also have some disadvantages: the glasses before two eyes alternately switch on/off state and it make eyes feel tired soon[3], and the shutter glasses are much more expensive and bulky than polarization glasses. To avoid all these unfavorable factors mentioned above, we use high-speed (120 Hz) LC polarization rotator before projection system to change images' polarization states, and the stereo images can be seen from general polarization glasses.

Besides, Xe lamps are used as light sources of projectors very popularly, whose lives are no more than 1 000 hours. Relatively, laser diodes (LD) can be used for more than 100 000 hours, and it has lots of advantages such as high brightness, large color gamut, and good polarization. However, the speckle limits the display application of the laser. Speckle are random spots with grainy structures arise in space when rough surface is illuminated with laser. The formation of speckle is due to coherent superimposition of all the wavelets emanating from the "random" rough surface[4], and it is regarded as noise that always reduces the images' quality. Several techniques have been proposed to remove speckle noise, such as a rotating diffuser[5,6], moving diffuser[7,8], moving screen[9,10] and some other approaches[11,12]. The use of rotating diffuser is well known as one speckle reduction method. A rotating diffuser produces variable random phase patterns sequentially at the diffusion point, so the objective speckle is averaged out on a screen. Although this method is effective in reducing objective speckle, it barely decreases subjective speckle that generates on the screen[13]. The reason for the remaining subjective speckle is that the speed of the phase modulation by using a rotating diffuser is not enough to eliminate the phase difference of surface height fluctuation. And mechanical principle has a major disadvantage that large area is needed[14]. Thus another speckle suppression method with small space and high efficiency is needed.

Based on LC polarization rotation characteristics, a novel single 3D laser projector is proposed, and laser is used as light source. By the use of rear projection screen and a vibrant diffuser, laser speckle limited to 0.1 can be achieved. Therefore, the movie-going experience can be hugely improved by using the proposed system.

As shown in Fig. 1, the 3D projection system is consisted of three parts: light source, projection system, and 3D control system.

The light source is comprised of three kinds of lasers. The red LD array is made up of four LDs (ML520G71, Mitsubishi, Japan) with wavelength of 632 nm which have an output of 300 mW each. The blue LD array is made up of two LDs (NDB7112E, Nichia, Japan) with wavelength of 450 nm which have an output of 500 mw each. Green laser is the combination of LD pumped Nd:YAG laser with wavelength of 1 064 nm and periodically poled lithium niobate (PPLN) for quasi-phase-matched second harmonic generation. It has an output of 1 000 mW with wavelength of 532 nm. Different mirrors reflect laser to the same

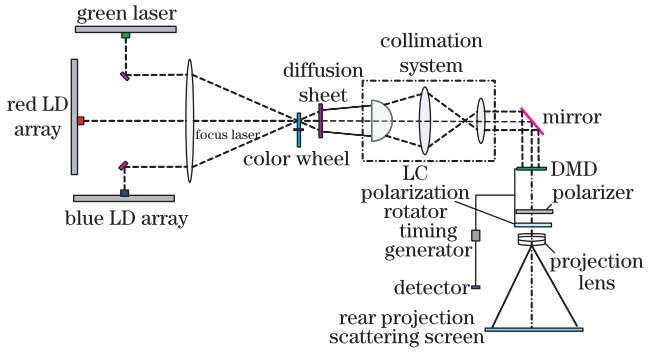

Fig. 1. Schematic diagram of 3D projection system. DMD: micro mirror derice.

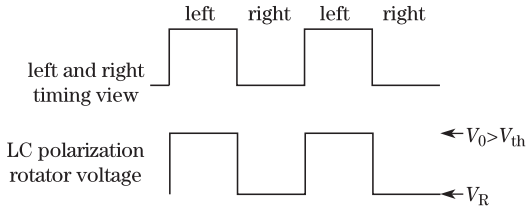

Fig. 2. Voltage timing diagram of LC polarization rotator.

direction of propagation, and laser is focused onto color wheel after passing through a large lens. The diffusion sheet makes the beam uniformity and then laser is illuminated onto digital micro-mirror device DMD chip with specified size (11.2×8.4 (mm)) after going through the collimation system. The DMD chip with digital light procession DLP-Link shutter display is made by TI corporation, whose resolution supports SVGA (800×600) and the size is 0.55 inch.

The DMD chip generates parallax images corresponding to left and right eyes with 120 Hz, and twisted nematic (TN) LC is used to change different polarization states of the parallax images. If threshold voltage V_0 is applied on LC, there is no phase changed; and if no voltage is applied, the polarization state will be changed at $\pi/2$. As shown in Fig. 2, when left eye image is projected, V_0 is applied on LC and polarization state is not changed; when right eye image is projected, no voltage is applied and thus the image's polarization state is changed with $\pi/2$. When the images are projected on screen with good polarization-maintaining quality, 3D images can be seen by people with polarization glasses.

The LC should be modulated with wide spectrum (from 380 to 700 nm). A tungsten halogen lamp (SPL-HL, Hangzhou SPI Photonics Co., Ltd, China) whose spectrum is from 360 to 2 500 nm is used to test the spectral characteristics of LC polarization rotator (shown in Fig. 3(a)). The light is turned into linearly polarization after passing through a polarizer, after going through LC and polarization analyzer which is vertical to the polarizer, the spectrum is measured by spectrometer (USB2000+UV-VISOcean Optics, USA). Particularly, we measure the transmission with three wavelengths (632, 532, and 450 nm) as shown in Fig. 3(b). In the chart we find that they have the close threshold voltage.

Silver screens are used widely for its good polarization-maintaining quality and high reflection efficiency. But they are very expensive and can't be used in rear projection. In order to overcome these disadvantages, a new acrylic screen with good polarization-maintaining quality is adopted. The measurement setup of polarization-maintaining characteristics is similar to the setup shown in Fig. 3(a) but the diffusive screen replaced LC between the polarizers.

Firstly, the laser transmission was test when light go through the two polarizer with different angles and it's drawn with square symbol in Fig. 4; then the screen was inserted between the polarizers and the polarization angle was changed, the result is drawn with round symbol in Fig. 4. It fits very well with Malus' law. From this figure, it can be seen that this screen has very good polarization-maintaining characteristics. The other feature of the screen is that it can reduce laser speckle for its body scattering. As shown in Fig. 5(a), there are lots of random grains whose sizes is between 2 and 15 μm in the screen. The relationship between laser speckle and reflective screen has been studied in many aspects[15−17], but the speckle theory in body scattering progresses much slower than surface scattering. This process is illustrated in Fig. 5(b), each light ray will go through different pathes for the random grain in the screen when laser beam illuminate into the screen.

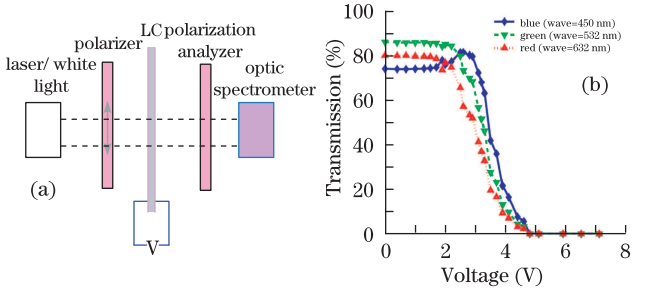

Fig. 3. (Color online) (a) Spectral characteristics of LC material testing; (b) transmission changed with voltage at three wavelengths.

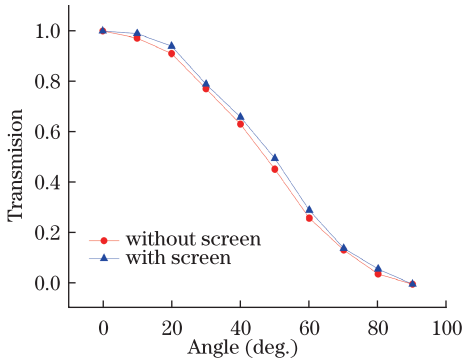

Fig. 4. (Color online) Polarization characteristics.

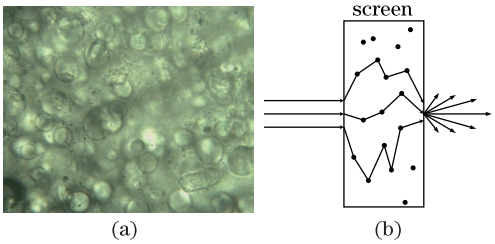

Fig. 5. (Color online) (a) The internal structure of rear projection screen shot by electron microscopy and (b) schematic diagram of laser passing through the screen.

The intensity contrast ratio is usually used to describe the degree of coherence of laser speckle:

$$C = \sigma_I / < I >, \tag{1}$$

where σ_I is the standard deviation and $< I >$is the average value of intensity over the speckle pattern. When the observation time is large relative to the coherence time of the light, the mean, $\mu_I =< I >$, and variance, $\sigma_I^2 =< I^2 > - < I >^2$, of the intensity of light having finite bandwidth can be expressed as[4]:

$$\sigma_I^2 = \int_0^\infty \int_0^\infty S(\lambda)S(\lambda')| < U_{\rm n}(x_i, y_i, \lambda) \times U_{\rm n}^*(x_i, y_i, \lambda') > |^2 {\rm d}\lambda{\rm d}\lambda' \mu_I(x_i, y_i), \tag{2}$$

$$= \int_0^\infty S(\lambda) < I_{\rm n}(x_i, y_i, \lambda) > d\lambda, \tag{3}$$

where $I_{\rm n}(x_i, y_i, \lambda) = U_{\rm n}(x_i, y_i, \lambda)U_{\rm n}^*(x_i, y_i, \lambda')$, $U_{\rm n}(x_i, y_i, \lambda)$ is the normalized spectral amplitude of the scalar (electric or magnetic) field at image position (x_i, y_i) at wavelength λ, $S(\lambda)$ is the power density of incident laser at wavelength λ from the source, and $< . . >$ is the expected value. The field at each point at the output of a scattering medium can be represented as a superposition of random phasors. Each random phasor can be considered as representing a random photon path through the medium. Within the image spot centered at (x_i, y_i), then

$$U(\lambda) = U_{\rm m}(\lambda) \exp(-i2\pi l/\lambda), \tag{4}$$

where l is the path-length random variable and $U_{\rm m}$ is the field-magnitude random variable and the phase $2\pi l/\lambda = \phi(\lambda)$ is uniformly distributed. Thus, within the small image spot, the mean intensity from Eq. (3) becomes

$$\mu_I = I_0 \int_0^\infty S(\lambda){\rm d}\lambda. \tag{5}$$

The normalized field probability density is

$$U_{\rm n}(\lambda) = I_{\rm n}^{1/2} \exp[-i\phi(\lambda)]. \tag{6}$$

The normalized field autocorrelation $\Gamma_U =< U_{\rm n}(\lambda)U_{\rm n}^*(\lambda') >$ can then be written as

$$\Gamma_U = I_0 < \exp[-i2\pi l(1/\lambda - 1/\lambda')] > . \tag{7}$$

When Eq. (7) is substituted into Eq. (2), and Eq. (5) is also used, the speckle contrast C becomes

$$\mu_I/\sigma_I = \int_0^\infty \left\{ \int_0^\infty \int_0^\infty S(\lambda)S(\lambda') \times | < \exp[-i2\pi l(1/\lambda - 1/\lambda')] > |^2 {\rm d}\lambda{\rm d}\lambda' \right\}^{1/2} / S(\lambda){\rm d}\lambda. \tag{8}$$

From Eq. (8), it can be seen that the speckle contrast will be reduced if l becomes larger.

Due to largest visual effect function of green color in the visible region[18], a diffuser with diameter of 1 cm is inserted in green laser's optical path. From Ref. [17], Goodman had proven that when laser passes through a changed diffuser, the speckle contrast can be reduced to $\sqrt{1/k}$, and

$$k = (d/s)^2, \tag{9}$$

where d is the diameter of eyes' distinguish primitive and s is the diameter of projection lens' distinguish primitive. Four independent dielectric elastomer actuators (DEAs) surround the diffuser. The thickness of DEAs will be changed if enough voltage is applied on them[19]. The four independent electrodes are used to obtain displacement of the diffuser in both directions of the x- and y-axis, as shown in Fig. 6. The equilibrium (no voltage applied on the electrodes) position of the diffuser is represented by the dashed circle. In Fig. 6(a) the x_1 and y_1 electrodes are activated, and the diffuser moves in positive x- and y-direction. In Figs. 6(b)–6(d) the analog effect is described for all four different states of the diffuser. After reaching state 6(d), the cycle continues with position 6(a). The moving frequency is 175 Hz and the amplitude is 0.5 mm.

By using of the vibrating diffuser and body scattering screen, laser speckle can be reduced to acceptable level. As shown in Fig. 7(a), images are projected on white paper directly and the speckle contrast is 0.25, in Fig. 7(b) images are projected onto body scattering screen and the speckle contrast is 0.15, and in Fig. 7(c) the diffuser is used and images are projected onto body scattering screen, the speckle contrast is 0.1.

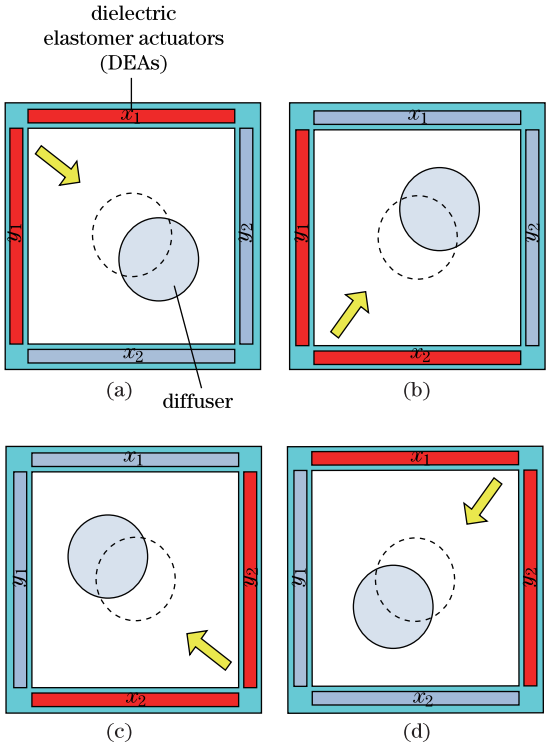

Fig. 6. (Color online) Illustration of four independent DEAs to move the diffuser.

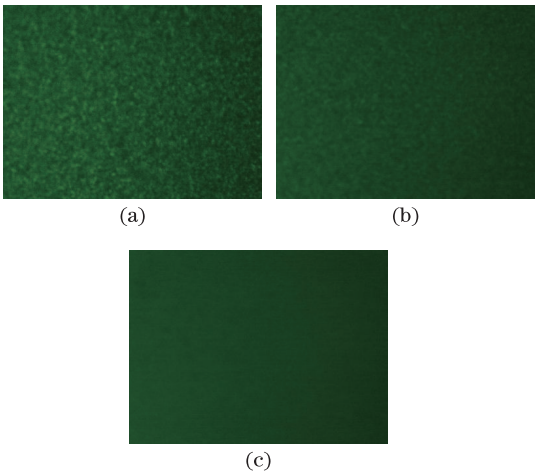

(a) (b) (c)

Fig. 7. (Color online) (a) Images are projected on white paper, (b) images are projected onto body scattering screen, and (c)the diffuser is used and images are projected onto body scattering screen.

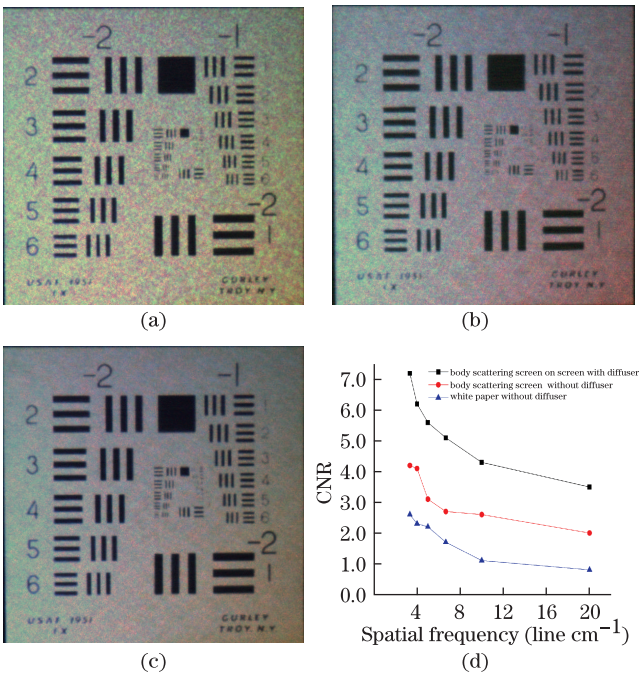

(a) (b) (c) (d)

Fig. 8. (Color online) (a) AF chart is imaged on white paper, (b) AF chart is imaged onto body scattering screen without diffuser, (c) AF chart is imaged onto body scattering screen with diffuser, and (d) CNR was plotted as a function of the spatial frequency of the features on the test chart.

Clearly, the phenomena of red and blue laser speckles are not severe in the proposed system, and it can be explained by the following two reasons: firstly, these two laser LDs are located in the form of array. From Ref. [17],

$$|\mu_{\rm A}|^2 = \exp[-(2\pi\sigma_{\rm h}/\lambda \bullet \Delta\theta_{\rm i}\sin\theta_{\rm i})] \qquad (10)$$

where $\mu_{\rm A}$ is cross-correlation between speckles illuminated from different angle of incidence, $\sigma_{\rm h}$ is standard deviation of surface roughness, $\theta_{\rm i}$ is the incidence angle, and $\Delta\theta_{\rm i}$ is the angle between different incidence angles. When $\Delta\theta_{\rm i}$ is only from 1° to 3°, $\mu_{\rm A}$ is approaching 0.1, which means different speckle is nearly irrelevant and can be reduced by the speckle patterns superimposed. Secondly, red and blue are both not sensitive to human's eyes and their visual effects functions are much smaller than green's[18]. Thus people can hardly distinguish these two kinds of speckle when they are projected onto the body scattering screen.

The image quality is the key point to projection system, we demonstrate that our system can prevent speckle to improve image quality. A 1951 US Air Force (AF) resolution test chart was imaged with the three conditions mentioned above. Image quality can be compared quantitatively using the contrast-to-noise ratio (CNR)[20,21], which is defined as

$$\mathrm{CNR} = (< I_{\rm f} > - < I_{\rm b} >)/((\sigma_{\rm f} + \sigma_{\rm b})/2), \qquad (11)$$

where $< I_{\rm f} >$ is the average intensity of the feature of interest (for example, a bar in the AF test chart), $< I_{\rm b} >$ is the average intensity of the surrounding background, and σ is the standard deviation of pixel intensity. The CNR describes the identifiability of a feature of interest in a given background. In the AF test chart, the bar's width decreases from 0.3 to 0.05 cm and the spatial frequency increases. As shown in Fig. 8(d), the CNR decreases with increasing spatial frequency. When the CNR approaches unity, feature contrast is comparable to image noise. Hence, speckle dramatically degrades image quality at high spatial coherence of laser. The collected images are presented in Figs. 8(a)–8(c). In Fig. 8(a), the laser exhibit speckle patterns within the AF charts, corrupts the image. When images are projected onto the body scattering screen, however, eliminate interference effects and produce a clean image of the object.

In conclusion, a new laser-based single 3D projector display system is demonstrated. The merit of the display system is its compactness and simplicity in construction. The key optical component in the system is a piece of TN LC with wide spectral transmission to rotate polarization, making it inexpensive to construct a 3D projector. Laser is used as light source because of its advantage in life, gamut, and brightness. With a novel diffusive screen which has good polarization-maintaining quality and a vibrant diffuser, laser speckle of the system can be reduced to 0.1 and image quality is also measured to show which is good enough for people to watch.

This research was supported by the Fundamental Research Funds for the Central Universities 09693.

References

1. J. Hoon, Y. Kim, H.-J. Choi, J. Hahn, J.-H. Park, H. Kim, S.-W. Min, N. Chen, and B. Lee, Appl. Opt. **50,** H87 (2011).
2. K. Iizuka, *Engineering Optics* (Springer Science+Business Media, 2008) chap. 16.
3. S. S. Kim, B. H. You, H. Choi, B. H. Berkeley, D. G. Kim, and N. D. Kim, SID Symposium Digest of Technical Papers **40,** 424 (2007).
4. J. C. Dainty, *Laser speckle and related phenomenon* (Springer-Verlag, Berlin and New York, 1984).
5. J. M. Florence, "Speckle-free display system using coherent light," U.S. Patent 5313479 (1994).

6. L. Wang, T. Tschudi, T. Halldórsson, and P. R. Pétursson, Appl. Opt. **37,** 1770 (1998).
7. J. I. Trisnadi, Proc. SPIE **4657,** 131 (2002).
8. S. Kubota and J. W. Goodman, Appl. Opt. **49,** 4385 (2010).
9. E. G. Rawson, A. B. Nafarrate, R. E. Norton, and J. W. Goodman, J. Opt. Soc. Am. **66,** 1290 (1976).
10. S. C. Shin, S. S. Yoo, S. Y. Lee, C.-Y. Park, S.-Y. Park, J. W. Kwon, and S.-G. Lee, Displays **27,** 91 (2006).
11. L. Wang, T. Tschudi, M. Boeddinghaus, A. Elbert, T. Halldórsson, and P. Pétursson, Opt. Eng. **39,** 1659 (2000).
12. V. Yurlov, A. Lapchuk, S. Yun, J. Song, and H. Yang, Appl. Opt. **47,** 179 (2008).
13. T. Uchida, Proc. IDW **9,** 1365 (2009).
14. I. N. Kompanets, A. L. Andreev, T. B. Andreeva, and M. V. Minchenko, SID Symposium Digest of Technical Papers **41,** 1065 (2010).
15. D. Brogioli, A. Vaolati, and M. Giglio, Appl. Phys. Lett. **81,** 4109 (2002).
16. J. W. Goodman, Proc. IEEE **53,** 1688 (1965).
17. J. W. Goodman, *Speckle phenomena in optics: theory and applications* (Ben Roberts & Company, Greenwood Village, 2007).
18. CIE (1932), *Commission Internationale de l'Eclairage Proceedings* (Cambridge University Press, Cambridge, 1931).
19. Y. Wei, Z. Feng, Y. liu, and D. zhang, J. Functional Materials and devices (in chinese) **12,** 501 (2006).
20. R. N. Bryan, *Introduction to the Science of Medical Imaging* (Cambridge University Press, Cambridge, 2009).
21. B. Redding, M. A. Choma, and H. Cao, Nature Photon. **6,** 355 (2012).